# Third-Order Elastic Moduli of Barium Fluoride*

D. GERLICH†
*Department of Physics and Materials Research Laboratory, University of Illinois, Urbana, Illinois*
(Received 1 November 1967; revised manuscript received 3 January 1968)

The complete set of the six third-order elastic moduli for $BaF_2$ was determined from the change in the sound velocity under hydrostatic and uniaxial pressure. The third-order elastic moduli for $BaF_2$ were found to be nonisotropic, although the second-order moduli are isotropic. The Grueneisen-mode $\gamma$'s and their low- and high-temperature limit were calculated from the third-order elastic moduli, as well as the isotherm ($P$-$V$ curve) over an extended pressure range. The experimental results for the third-order elastic moduli were compared with theoretically calculated values, and good agreement was found.

## I. INTRODUCTION

THERE has been a growing interest over the last few years in the anharmonic properties of solids, due, on the one hand, to the increasing amount of experimental data becoming available, and, on the other hand, to progress in theoretical interpretation of anharmonicity effects in solids.[1] The third-order elastic (T.O.E.) moduli of several of the alkali halides have been measured experimentally, and computed theoretically.[2–4] All these substances are ionic crystals, possessing a lattice in which every ion is a center of inversion. Thus, the theoretical calculations, which are based on a central-force model, will yield a set of T.O.E. moduli obeying the Cauchy relations.[5] The experimental data, where the complete set of the T.O.E. has been measured, do obey fairly well the Cauchy relations.[2]

The fluorite structure is probably one of the simplest nonprimitive crystalline lattices. Thus the study of the T.O.E. moduli of an ionic crystal with such a structure should be of interest. It might elucidate, perhaps, the question of the applicability of the central-force model, and the Cauchy relations to the fluorite structure.

Barium fluoride is an interesting material, being an isotropic single crystal as far as its second-order elastic (S.O.E.) moduli are concerned.[6] It is of interest, therefore, to investigate its T.O.E. moduli in order to examine whether the latter are isotropic as well, and whether the Cauchy relations are satisfied. With this in mind, the present investigation was undertaken. The complete set of the T.O.E. moduli for $BaF_2$ was determined, and a comparison with theoretically computed values was made.

## II. EXPERIMENTAL

The samples used in the present work were single crystals of $BaF_2$, purchased from the Harshaw Chemical Co. They were in the shape of cubes, edges approximately $15\times16\times17$ mm, the cube faces corresponding to (110), (1$\bar{1}$0), and (001) crystalline planes. The orientations of the faces were checked by means of x-ray Laue back reflections, and were found to correspond to the specified crystalline plane within $\frac{1}{2}$ deg. The crystals were hand lapped flat to a few $\mu$in., and parallel to a few parts in $10^5$.

Barium fluoride, being a cubic crystal, has six independent T.O.E. moduli, $C_{111}$, $C_{112}$, $C_{144}$, $C_{166}$, $C_{123}$, and $C_{456}$. The Thurston-Brugger definitions of the T.O.E. moduli[7] are used throughout the present paper. These moduli were determined from the variation of the sound velocity under hydrostatic pressure, and uniaxial compression. Fourteen different combinations of propagation modes and stresses could be used.[7] These were (a) the five different propagation modes under hydrostatic pressure, (b) the six different modes under uniaxial compression in the [1$\bar{1}$0] direction, and (c) the three different modes under uniaxial compression in the [001] direction. These measurements provide 14 equations for the T.O.E. moduli, from which the latter were computed by means of a least-squares fit. The sound waves were generated by means of $X$ and $AC$ cut crystalline quartz transducers, bonded to the sample with Nonaq stopcock grease.

In order to avoid cracking the samples, and to eliminate dislocation-lines movement, which might completely falsify the T.O.E. moduli measurements,[2,8,9] the uniaxial compression had to be kept at a low level; it had never exceeded 35 kg/cm$^2$ in our measurements. In addition, the crystals were irradiated with a $\gamma$-ray dose of about 3000 R, in order to provide additional pinning centers for the dislocation lines, and thus hindering their movement.[2,10]

As a result of the low uniaxial compression level, an experimental method possessing a very high sensitivity had to be used. It is essentially a McSkimin frequency

* Work supported in part by the U. S. Atomic Energy Commission under Contract No. AT(11-1)-1198: Report No. COO-1198-489.
† Permanent address: Physics Dept., Tel-Aviv University, Ramat Aviv, Israel.
[1] G. Leibfried and W. Ludwig, *Solid State Physics*, edited by F. Seitz and D. Turnbull (Academic Press Inc., New York, 1961), Vol. 12.
[2] K. D. Swartz, J. Acoust. Soc. Am. **41**, 1083 (1967).
[3] P. B. Ghate, Phys. Rev. **139**, A1666 (1965).
[4] K. M. Koliward, P. B. Ghate, and A. L. Ruoff, Phys. Status Solidi **21**, 507 (1967).
[5] M. Born and K. Huang, *Dynamical Theory of Crystal Lattices* (Clarendon Press, Oxford, England, 1954).
[6] D. Gerlich, Phys. Rev. **135**, A1331 (1964).
[7] R. N. Thurston and K. Brugger, Phys. Rev. **133**, A1604 (1964).
[8] Y. Hiki and A. V. Granato, Phys. Rev. **144**, 411 (1966).
[9] K. Salama and G. A. Alers, Phys. Rev. **161**, 673 (1967).
[10] R. Gordon and A. S. Nowick, Acta Met. 4, 514 (1956).

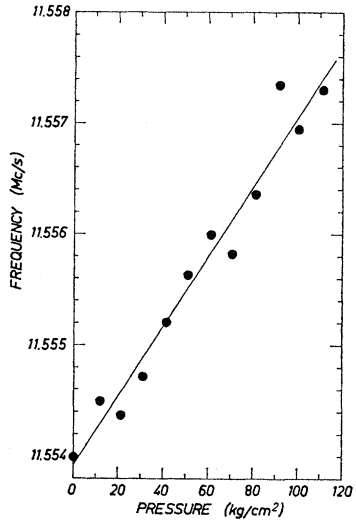


FIG 1. Change in frequency versus hydrostatic pressure for a longitudinal sound wave propagating in the [001] direction.

modulated pulse-superposition method,[11–13] using a cw carrier wave, set up by J. Holder of this laboratory.

The changes in the sound velocity with pressure were determined by measuring the resonant frequency closest to the free transducer resonant frequency as a function of pressure. If the bond does not change with pressure, then the sound travel time is inversely proportional to the frequency.[12] The temperature of the sample was monitored carefully at all times, and all measurements were standardized to the same temperature.

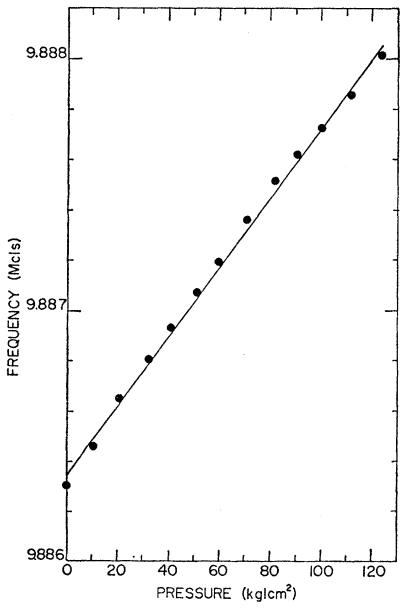


FIG. 2. Change in frequency versus hydrostatic pressure for a shear sound wave propagating in the [001] direction, polarized in the (001) plane.

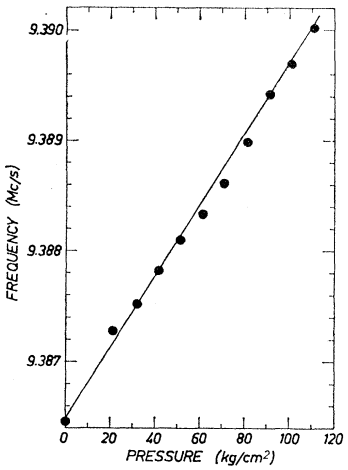


FIG. 3. Change in frequency versus hydrostatic pressure for a longitudinal sound wave propagating in the [110] direction.

The hydrostatic pressure was generated by tank nitrogen gas, and the pressure was measured by means of a factory calibrated Heise-Bourdon gauge. The uniaxial compression was generated with a Tinius-Olsen loading machine, the stress being determined by a calibrated load cell. Indium metal shims were placed between the sample and the pressurizing surfaces in order to eliminate shear stresses being applied to the sample faces under uniaxial compression.

## III. RESULTS

All measurements were made at room temperature, and all results were normalized to 295°K. Figures 1–5 show the change in resonant frequency with hydrostatic pressure for the five different propagation modes. It is interesting to note that the changes are negative, namely, the sound velocity decreases with increasing

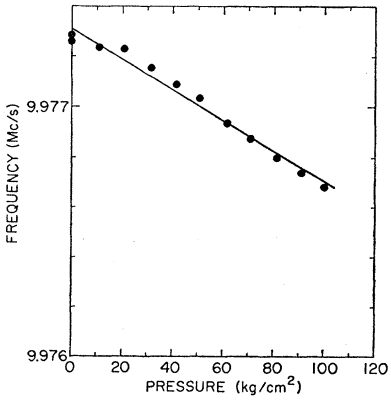


FIG. 4. Change in frequency versus hydrostatic pressure for a shear sound wave propagating in the [110] direction, polarized in the [110] direction.

[11] H. J. McSkimin, J. Acoust. Soc. Am. 33, 12 (1961).
[12] H. J. McSkimin and P. Andreatch, Jr., J. Acoust. Soc. Am. 34, 609 (1962).
[13] H. J. McSkimin and P. Andreatch, Jr., J. Acoust. Soc. Am. 41, 1052 (1967).

pressure, for the $\frac{1}{2}(c_{11}-c_{12})$ mode. A similar behavior was found in KF for the $c_{44}$ mode.[4] In Figs. 6 and 7 the resonant frequency changes as a function of the applied uniaxial compression in the $[1\bar{1}0]$ and [001] directions are shown. As can be seen, in all cases the frequency, and hence the velocity, changes were linear up to the highest pressure used, which is a necessary condition for no dislocation-lines movement to have occurred. The straight lines in Figs. 1–7 are least-squares fits to the experimental data. From the slopes of these lines, the pressure derivatives at zero pressure of $\rho_0W^2$, $[(\rho_0W^2)_{p=0}']$, are determined. Here $\rho_0$ is the zero pressure density, $W$ is the natural velocity, defined as $2L_0/\tau$, where $L_0$ is the zero-pressure length of the sample and $\tau$ is the round-trip travel time of the sound through the sample. The values of the various $(\rho_0W^2)_{p=0}'$ determined from the straight lines in Figs. 1–7, with their associated errors, are shown in Table I.

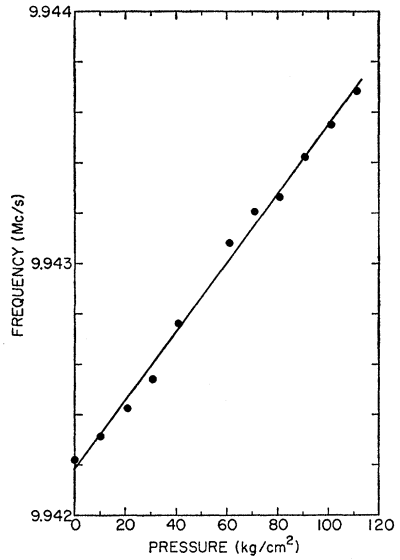


FIG. 5. Change in frequency versus hydrostatic pressure for a shear sound wave propagating in the [110] direction, polarized in the [001] direction.

In order to compute the T.O.E. moduli from the measured $(\rho_0W^2)_{p=0}'$, the values of the isothermal and adiabatic S.O.E. moduli are required. The adiabatic S.O.E. moduli were determined by measuring the sound velocity in the five different propagation modes, and computing the S.O.E. moduli by a least-squares fit. The results are presented in Table II. The isothermal moduli were computed from the values of the adiabatic ones, using the room-temperature thermal expansion and specific-heat data.[14,15]

From the experimentally determined S.O.E. moduli, and the various $(\rho_0W^2)_{p=0}'$, the six T.O.E. moduli can

[14] A. C. Bailey and B. Yates, Proc. Phys. Soc. (London) **91**, 390 (1967).

[15] K. S. Pitzer, W. V. Smith, and W. M. Latimer, J. Am. Chem. Soc. **60**, 1826 (1938).

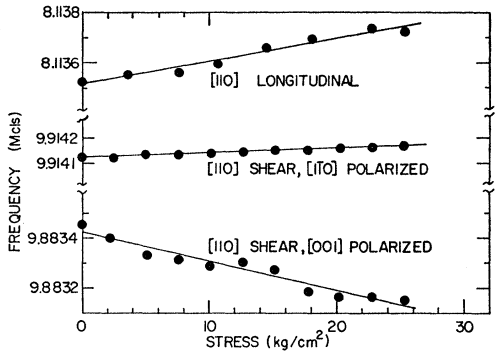


FIG. 6. Change in frequency versus uniaxial compression along the [001] direction for different propagation modes.

now be computed. But, it should first be ascertained that no dislocation motion has occurred during the uniaxial compression. This is done by calculating the three linear combinations of the T.O.E. moduli which are determined from the hydrostatic measurements alone, namely, $C_{111}+2C_{112}$, $C_{144}+2C_{166}$, and $2C_{112}+C_{123}$, separately from the uniaxial and hydrostatic runs. These three linear combinations were determined for the uniaxial runs alone, by solving the set of the appropriate nine linear equations in the six T.O.E. moduli by a least-squares fit. From the individual T.O.E. moduli computed, the above three linear combinations were determined. Since no dislocation motion should occur during the hydrostatic runs, a comparison of the two sets of data should show whether such motion has occurred

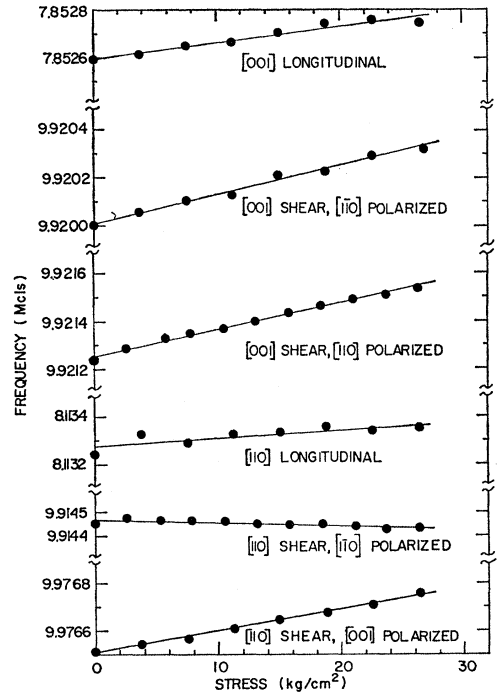


FIG. 7. Change in frequency versus uniaxial compression along the $[1\bar{1}0]$ direction for different propagation modes.

TABLE I. Value of $(\rho_0 W^2)_{p=0}'$ for the different propagation modes.

| Propagation direction | Displacement direction | Stress direction | $(\rho_0 W^2)_{p=0}'$ |
|---|---|---|---|
| [110] | [110] | [001] | 2.02 ±0.14 |
| [110] | [1$\bar{1}$0] | [001] | 0.0978±0.0074 |
| [110] | [001] | [001] | −0.599 ±0.047 |
| [001] | [001] | [1$\bar{1}$0] | 1.55 ±0.11 |
| [001] | [1$\bar{1}$0] | [1$\bar{1}$0] | 0.620 ±0.030 |
| [001] | [110] | [1$\bar{1}$0] | 0.571 ±0.023 |
| [110] | [110] | [1$\bar{1}$0] | 0.70 ±0.15 |
| [110] | [1$\bar{1}$0] | [1$\bar{1}$0] | −0.077 ±0.014 |
| [110] | [001] | [1$\bar{1}$0] | 0.458 ±0.017 |
| [001] | [001] | hydrostatic | 4.96 ±0.31 |
| [001] | (001) plane | hydrostatic | 0.711 ±0.021 |
| [110] | [110] | hydrostatic | 6.02 ±0.17 |
| [110] | [1$\bar{1}$0] | hydrostatic | −0.315 ±0.017 |
| [110] | [001] | hydrostatic | 0.701 ±0.025 |

under uniaxial compression. These two sets of data with their errors are presented in Table III. As can be seen, the agreement between the two sets of data is within the limit of error, indicating that no dislocation motion has occurred during the uniaxial runs.

From the complete set of experimental data, hydrostatic and uniaxial, the six independent T.O.E. moduli are now determined by means of a least-squares fit, the results being shown in Table IV.

The estimate of the errors is done as follows. The errors in the different $(\rho_0 W^2)_{p=0}'$ are computed by calculating the standard deviation from the experimental data and setting the error as 0.675 times the standard deviation. In this way the errors shown in Table I were determined. The T.O.E. moduli are determined by

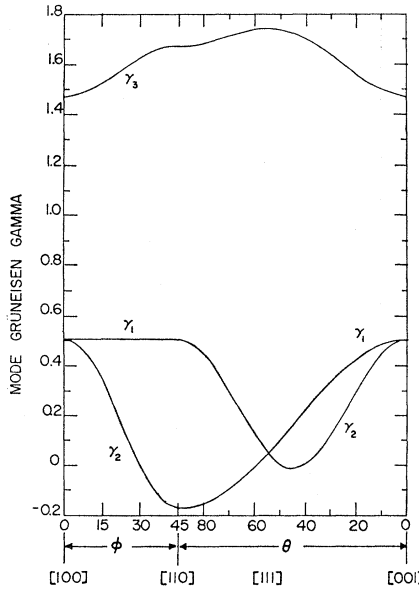


FIG. 8. The three mode $\gamma$'s as a function of the crystalline direction.

TABLE II. Second-order abiabatic elastic moduli for $BaF_2$ (units are $10^{11}$ dyn/cm$^2$).

| $c_{11}^S$ | $c_{12}^S$ | $c_{44}$ |
|---|---|---|
| 8.948 | 3.854 | 2.495 |

solving a set of linear equations of the form

$$\|A\|\times\|C\|=\|B\|,$$

where $\|A\|$ is a matrix whose elements are either constants, or depend only on the S.O.E. moduli. $\|C\|$ is the column matrix of the T.O.E. moduli, and $\|B\|$ is the column matrix whose elements are linear functions of the various $(\rho_0 W^2)_{p=0}'$. Since the errors in the S.O.E. moduli are negligible compared to the errors in the $(\rho_0 W^2)_{p=0}'$, the errors in the T.O.E. moduli can be determined from the set of equations

$$\|A\|\times\|\Delta C\|=\|\Delta B\|,$$

where $\|\Delta C\|$ is a column matrix of the errors in the T.O.E. moduli and $\|\Delta B\|$ is a column matrix of the errors in the elements of $\|B\|$ determined from the errors in the $(\rho_0 W^2)_{p=0}'$. In such a manner, the errors shown in Tables III and IV were calculated.

## IV. DISCUSSION

As has already been mentioned, $BaF_2$ is isotropic as far as the S.O.E. moduli are concerned.[6] It is obvious that the isotropy relations for the T.O.E. moduli[7]

$$C_{111}=C_{123}+6C_{144}+8C_{456},$$
$$C_{112}=C_{123}+2C_{144},$$
$$C_{166}=C_{144}+2C_{456},$$

are not satisfied. This can be seen from Table V, where the values of the various ratios of the S.O.E. and T.O.E. moduli, which should equal unity in an isotropic material, are shown. It therefore seems that $BaF_2$ is not inherently isotropic, the isotropy of the S.O.E. moduli being accidental. This is probably caused by the fact that the form of the strain energy function is such as to make $\frac{1}{2}(c_{11}-c_{12})$ equal to $c_{44}$.

The pressure derivatives of the S.O.E. moduli of $CaF_2$ have recently been measured.[16,17] In Table VI the values of the room-temperature pressure derivatives

TABLE III. $C_{111}+2C_{112}$, $C_{144}+2C_{166}$, and $2C_{112}+C_{123}$ as determined separately from hydrostatic and uniaxial runs (units are $10^{11}$ dyn/cm$^2$).

| | $C_{111}+2C_{112}$ | $C_{144}+2C_{166}$ | $2C_{112}+C_{123}$ |
|---|---|---|---|
| Hydrostatic | −115.0± 4.4 | −32.9±0.12 | −82.8±2.5 |
| Uniaxial | −126.0±12.5 | −29.1±1.2 | −84.6±7.6 |

[16] C. Wong and D. E. Schuele, J. Phys. Chem. Solids **28**, 1225 (1967).
[17] P. S. Ho and A. L. Ruoff, Phys. Rev. **161**, 864 (1967).

TABLE IV. Third-order elastic moduli of $BaF_2$ (units are $10^{11}$ dyn/cm$^2$).

| $C_{111}$ | $C_{112}$ | $C_{144}$ | $C_{166}$ | $C_{123}$ | $C_{456}$ |
|---|---|---|---|---|---|
| $-58.4\pm1.5$ | $-29.9\pm1.4$ | $-12.1\pm0.3$ | $-8.89\pm0.19$ | $-20.6\pm1.1$ | $-2.71\pm0.01$ |

of $CaF_2$ and $BaF_2$ are compared. Here $C_L$, $C'$, and $C$ are $\rho v^2$, where $v$ is the sound velocity for the longitudinal and the two shear waves in the [110] direction. As can be seen, the pattern of the numbers for the two substances is similar.

From the pressure derivatives, the Grueneisen-mode $\gamma$'s $\gamma_i$, as well as the low- and high-temperature limit of the thermodynamic Grueneisen $\gamma$'s $\gamma_L$ and $\gamma_H$ can be determined.[18] Utilizing Schuele's computer program,[18] the $\gamma_i$'s and $\gamma_L$ and $\gamma_H$ have been determined from the pressure derivatives of the S.O.E. moduli for $BaF_2$. The $\gamma_i$'s for a few selected directions are shown in Fig. 8. Here 1 is the slow-shear mode, 2 is the fast-shear mode, and 3 is the longitudinal mode. As can be seen, $\gamma_2$ becomes negative over some directions, namely, for these directions the frequencies, and hence the velocities of the fast-shear mode decrease with decreasing volume. The $\gamma_L$ and $\gamma_H$ determined from the elastic data are compared with the values determined from thermal-expansion measurements[14] in Table VII. As can be seen, the disagreement for $\gamma_H$ is much larger than for $\gamma_L$, the elastic $\gamma_H$ being lower than the thermal-expansion value. This situation might arise when the contribution of the optical modes to the $\gamma_i$'s becomes significant. Such a case is especially probable with some $\gamma_i$'s going negative,[18] as is the case for $BaF_2$. There is the possibility, although this is not very likely, that the discrepancy for the $\gamma_L$'s, is caused by the fact that the elastic value renders the value of $\gamma$ at 0°K, while the thermal value was computed from 20°K data.

From the pressure derivatives of the bulk modulus, the isotherm for the material over a wide pressure range can be evaluated.[19] In Fig. 9, the room-temperature isotherm for pressures up to 200 kbar is shown.

R. Srinivasan[20,21] has made a theoretical calculation of the T.O.E. moduli for the fluorite structure. His calculations were carried out for two models, a rigid-ion model,[5] and a dipole-shell model.[22] A central-force interaction was assumed, consisting of an electrostatic Coulombic and a repulsive contribution. The latter was assumed between first-neighbor metal-halogen and second neighbor halogen-halogen ions. The values of the T.O.E. moduli computed theoretically by Srinivasan[21] based on the above models are shown in Table VIII. It is evident that the agreement between the experimental results and the theoretical calculations is very gratifying. This indicates that the simple central-force model is also applicable to the fluorite structure. The reason for the Cauchy relations

$$C_{112}=C_{166} \quad C_{123}=C_{144}=C_{456}$$

TABLE V. Isotropy relations for the S.O.E. and T.O.E. moduli of $BaF_2$ at room temperature.

| $\frac{2c_{44}}{c_{11}-c_{12}}$ | $\frac{C_{123}+6C_{144}+8C_{456}}{C_{111}}$ | $\frac{C_{123}+2C_{144}}{C_{112}}$ | $\frac{C_{144}+2C_{456}}{C_{166}}$ |
|---|---|---|---|
| 1.03 | 1.97 | 1.50 | 1.97 |

TABLE VI. Comparison of the pressure derivatives of the second-order elastic moduli for $CaF_2$ and $BaF_2$.

| | $\partial C_L/\partial p$ | $\partial C'/\partial p$ | $\partial C/\partial p$ |
|---|---|---|---|
| $CaF_2$ (Wong and Schuele) | 6.49 | 0.847 | 1.30 |
| $CaF_2$ (Ho and Ruoff) | 7.68 | 0.27 | 1.33 |
| $BaF_2$ (Present work) | 6.40 | 0 | 0.685 |

TABLE VII. Comparison of the values of $\gamma_L$ and $\gamma_H$ from elastic and thermal-expansion data.

| | $\gamma_L$ | $\gamma_H$ |
|---|---|---|
| Elastic | $0.38\pm0.03$ | $0.77\pm0.05$ |
| Thermal expansion | 0.27 (20°K) | 1.57 (270°K) |

TABLE VIII. Values of the theoretically calculated third-order elastic moudli for $BaF_2$ (units are $10^{11}$ dyn/cm$^2$).

| | $C_{111}$ | $C_{112}$ | $C_{114}$ | $C_{166}$ | $C_{123}$ | $C_{456}$ |
|---|---|---|---|---|---|---|
| Rigid-ion model | −47.0 | −32.9 | −8.5 | −14.2 | −32.1 | −0.7 |
| Dipole-shell model | −47.0 | −32.9 | −5.3 | −12.9 | −23.1 | −1.7 |
| Experimental results | −58.4 | −29.9 | −12.1 | −8.9 | −20.6 | −2.7 |

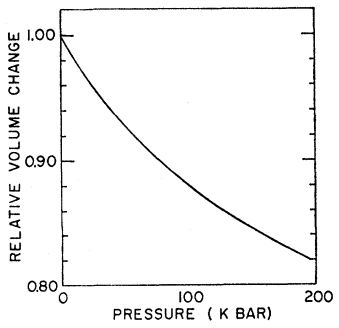


FIG. 9. Room temperature isotherm for $BaF_2$.

[18] D. E. Schuele and C. S. Smith, J. Phys. Chem. Solids **25**, 801 (1964).

[19] O. L. Anderson, J. Phys. Chem. Solids **27**, 547 (1966).

[20] R. Srinivasan, Bull. Am. Phys. Soc. **12**, 305 (1967).

[21] R. Srinivasan (private communication).

[22] J. D. Axe, Phys. Rev. **139**, A1215 (1965).

not being satisfied in the case of $BaF_2$ must therefore be due to the relative movement of the various sublattices in the fluorite structure under strain, and not to the action of many-body forces. Such an internal displacement will cause a deviation from the Cauchy relations even in a central-force model.

## ACKNOWLEDGMENTS

The author wishes to express his indebtedness to the Department of Physics, and the Materials Research Laboratory, University of Illinois, for a summer appointment, during the tenure of which this work was carried out. He wishes also to express his deep gratitude to Professor A. V. Granato for his hospitality, which enabled this work to be done, and for many helpful suggestions and discussions, and for a critical reading of the manuscript. Thanks are also due to T. Suzuki and J. Thomas for many helpful discussions concerning the theory of third-order elastic moduli, to J. Holder for the loan of the measuring equipment, to T. Ochs for technical assistance, and to Dr. R. Srivinasan for communicating his results prior to publication.

PHYSICAL REVIEW VOLUME 168, NUMBER 3 15 APRIL 1968

# Lattice Dynamics of Microcrystallites

L. S. KOTHARI AND C. M. SINGAL*
*Department of Physics and Astrophysics, University of Delhi, Delhi, India*
(Received 31 October 1967)

We have calculated the allowed frequency modes for simple cubic microcrystallites with free boundaries, taking the nearest-neighbor interaction. The mean-square displacement (m.s.d.) and the mean-square velocities (m.s.v.) in different directions, for atoms in different positions on the lattice, have been evaluated. Two different sets of force constants have been used. We find that for surface atoms, m.s.d. for motion along the surface is nearly the same as for motion perpendicular to the surface. m.s.d. is maximum for corner atoms and minimum for atoms in bulk. On the other hand, m.s.v. is maximum for atoms in bulk and minimum for corner atoms. At any fixed site, we find that both m.s.d. and m.s.v. increase with increasing crystal size, and tend to an asymptotic value. For one set of force constants we have also calculated the specific heat of microcrystallites at various temperatures, as a function of crystallite size. The effective Debye temperature is estimated, and its variation, both with crystallite size and sample temperature, is discussed.

## INTRODUCTION

RECENTLY, a lot of theoretical and experimental work have been reported on the surface vibrations of crystals.[1–8] Most of the theoretical work has been done on the vibrations of thin slabs of infinite extension in two dimensions.[1–4] The case of small crystallites has also been considered, but here most of the work has been phenomenological.[9–15] Recently, vibrations of a small linear chain with free ends have been investigated.[8]

Jones, McKinney, and Webb[5] have studied the reflection of electrons from the (111) surface of a silver crystal and have determined the mean-square displacements (m.s.d.)[4] normal to the crystal surface of atoms at different depths in the crystal. At the surface the m.s.d. is $2.0\pm0.2$ times larger than in the bulk, and the amplitude approaches the bulk value nearly as $e^{-n}$, where $n$ labels the planes starting from the surface layer. Measurements of thermal displacements in other directions indicate that they are nearly isotropic. This result is in disagreement with the theoretical calculations of Maradudin and Melngailis,[2] and of Clark, Herman, and Wallis.[1] Maradudin and Melngailis have shown that in the case of a simple cubic crystal with nearest- and next-nearest-neighbor central-force interactions between atoms, in the high-temperature limit (i.e., to lowest order in inverse temperature) for a surface atom, the m.s.d. perpendicular to the surface is at most twice its value in bulk, whereas the m.s.d. parallel to the surface is only about 30% larger than the bulk value. Similar anisotropy in the m.s.d. is found by Clark, Herman, and Wallis for surface atoms

* Present address: Physics Dept., Hansraj College, Delhi-7, India.
[1] B. C. Clark, R. Herman, and R. F. Wallis, Phys. Rev. **139**, A860 (1965).
[2] A. A. Maradudin and J. Melngailis, Phys. Rev. **133**, A1188 (1964).
[3] M. Rich, Phys. Letters **4**, 153 (1963).
[4] R. F. Wallis and D. C. Gazis, Phys. Rev. **128**, 106 (1962).
[5] E. R. Jones, J. T. McKinney, and M. B. Webb, Phys. Rev. **151**, 476 (1966).
[6] J. Aldag and R. M. Stern, Phys. Rev. Letters **14**, 857 (1965).
[7] A. U. Mac Rae and L. H. Germer, Phys. Rev. Letters **8**, 489 (1962).
[8] John R. Clem and Robert P. Godwin, Am. J. Phys. **34**, 460 (1966).
[9] T. H. K. Barron, W. T. Berg, and J. A. Morrison, Proc. Roy. Soc. (London) **A250**, 70 (1960).
[10] F. V. Hunt, L. L. Beranek, and D. Y. Maa, J. Acoust. Soc. Am. **11**, 80 (1939).
[11] D. Y. Maa, J. Acoust. Soc. Am. **10**, 235 (1939).
[12] R. H. Bolt, J. Acoust. Soc. Am. **10**, 228 (1939).
[13] H. B. Rosenstock, J. Chem. Phys. **23**, 2415 (1950).
[14] E. W. Montroll, J. Chem. Phys. **18**, 183 (1950).
[15] M. Dupuis, R. Mazo, and L. Onsager, J. Chem. Phys. **33**, 1452 (1960).